Diverging the anthracycline class of anti-cancer drugs for superior survival of acute myeloid leukemia patients

Xiaohang Qiao,[1,2,*,†] Sabina Y. van der Zanden,[3,*] Xiaoyang Li,[4,*] Minkang Tan,[3] Yunxiang Zhang,[4] Ji-Ying Song,[6] Merle A. van Gelder,[3] Feija L. Hamoen,[3] Lennert Janssen,[3] Charlotte L. Zuur,[1,2] Baoxu Pang,[3] Olaf van Tellingen,[5] Junmin Li,[4,†] and Jacques Neefjes[3,†]

[1]Division of Tumor Biology and Immunology, The Netherlands Cancer Institute, Amsterdam, The Netherlands;
[2]Department of Head and Neck Oncology and Surgery, The Netherlands Cancer Institute, Amsterdam, The Netherlands;
[3]Department of Cell and Chemical Biology, ONCODE Institute, Leiden University Medical Center, Leiden, The Netherlands;
[4]Shanghai Institute of Hematology, State Key Laboratory of Medical Genomics, National Research Center for Translational Medicine, Ruijin Hospital affiliated to Shanghai Jiao Tong University School of Medicine, Shanghai, China;
[5]Division of Pharmacology, The Netherlands Cancer Institute, Amsterdam, The Netherlands;
[6]Division of Experimental Animal Pathology, The Netherlands Cancer Institute, Amsterdam, The Netherlands;
*These authors contributed equally to this work.

[†]Correspondence: email: x.qiao@nki.nl; drlijunmin@126.com; j.j.c.neefjes@lumc.nl

Key words:

Anthracycline, Doxorubicin, Aclarubicin, Acute Myeloid Leukemia, Cardiotoxicity, Histone Eviction, Bio-distribution, Cross-resistance

Abstract

The efficacy of anthracycline-based chemotherapeutics, which include doxorubicin and its structural relatives daunorubicin and idarubicin, remains almost unmatched in oncology, despite a side effect profile including cumulative dose-dependent cardiotoxicity, therapy-related malignancies and infertility. Detoxification of anthracyclines while preserving their anti-neoplastic effects is arguably a major unmet need in modern oncology, as cardiovascular complications that limit anti-cancer treatment are now a leading cause of morbidity and mortality among the 17 million cancer survivors in the U.S.. To address this, we examined different clinically relevant anthracycline drugs with respect to a series of features including mode of action (chromatin and DNA damage), bio-distribution, anti-tumor efficacy and cardiotoxicity in pre-clinical models and patients. We show that different anthracycline drugs have surprisingly individual efficacy and toxicity profiles. In particular, aclarubicin stands out in pre-clinical models and clinical trials as it potently kills cancer cells, does not induce therapy-related malignancies or cardiotoxicity, and can be safely administered even after a maximum cumulative dose of either ida- or doxorubicin has been reached. Retrospective analysis of aclarubicin used in second-line treatment of relapsed/refractory AML patients showed similar survival effects to its use in first line, leading to an almost 25% increase in 5-year overall survival. Considering individual anthracyclines as different drugs provides new treatment options that strongly improve survival of cancer patients while limiting the toxic side-effects.

Introduction

Most anthracyclines function as poisons of the enzyme topoisomerase II (TopoII) that trap it on chromatin and thus induce DNA double-strand breaks (DSBs) [1]. In addition, these drugs also evict histones from defined genomic areas, which results in delayed DNA damage repair

and epigenetic and transcriptomic alterations, collectively termed chromatin damage [2-4]. Histone eviction appears to be a major cytotoxic activity of anthracyclines [5]. TopoII poisons, like etoposide, that only generate DSBs are considerably less effective in cancer treatment [2, 6], and also less toxic [5, 7]. On the contrary, aclarubicin only induces histone eviction and is highly effective in treating *de novo* acute myeloid leukemia (AML) [5]. Hence, DNA damage appears not to be a prerequisite for effective anti-cancer activities. Removing DNA damage from chromatin damage activity mitigates cardiotoxicity and therapy-related tumorigenesis of anthracyclines, without hampering their anti-cancer effect [5]. Clinical application of detoxified anthracyclines will confer major benefits in cancer therapy, expanding treatment options for patients with comorbidities including older adults [8] and reducing late effects, particularly for pediatric patients [9]. Detoxified anthracyclines would enable chronic treatment of cancer, while the current toxic anthracyclines only allow for limited treatment due to cumulative dose-dependent cardiotoxicity risk. Here, we systematically evaluated anthracycline drugs currently used in clinic against a series of key features to determine whether they differ in terms of anti-neoplastic potency, site of action and toxicity profiles. We identified aclarubicin, currently used only in Asia for AML patients with high comorbidity indices, as an anthracycline variant that lacks cardiotoxicity side effects and can be used after maximum dose of doxo- or ida in mice and men. Aclarubicin-based therapy increases the overall survival of relapsed/refractory AML patients by almost 25%. These data illustrate how aclarubicin can transform leukemia treatment for children, unfit adults and relapsed/refractory AML patients that currently have a poor prognosis, addressing a major unmet need in current oncology practice.

Materials and methods

Reagents

Doxorubicin and etoposide were purchased from Pharmachemie (The Netherlands), daunorubicin was obtained from Sanofi-Aventis and epirubicin was obtained from Accord Healthcare Limited (UK), idarubicin was obtained from Pfizer and Santa Cruz Biotechnology (sc-204774). Aclarubicin for in vivo mouse experiments was obtained from Shenzhen Main Luck Pharmaceuticals Inc. Aclarubicin (for in vitro experiments, sc-200160) and amrubicin (sc-207289) were obtained from Santa Cruz Biotechnology.

Cell culture

K562, MM6, MOLM13, MV4:11, and U937 and THP-1 were cultured in RPMI-1640 medium supplemented with 8% fetal calf serum (FCS). OCI-AML2 and OCI-AML3 and OCI-AML4 were cultured in Iscove's Modified Dulbecco's medium (IMDM) supplemented with 8% FCS and glutamine. MelJuSo cells were maintained in IMDM supplemented with 8% FCS. All cell lines were maintained in a humidified atmosphere of 5% CO_2 at 37 °C, regularly tested for the absence of mycoplasma and STR profile identified.

Cell line construction

For endogenous tagged GFP-H2B K562 cells, mScarlet was swapped for GFP in the homology repair construct using NheI and BglII and cells were generated as described [5]. Co-transfection into K562 cells was done by electroporation using Lonza SF cell line kit. ABCB1 overexpressing K562 cells were generated as described [10]. Endogenous tagged 3×Flag-TopoIIα K562 cell line was generated using HR-3×Flag construct designed at least 40 base pairs up and downstream of the genomic TopoIIα stop codon. The gRNA target sequence was designed using the ZANG Lab CRISPR tool (http://crispr.mit.edu/) and cloned into the pX330 vector. Primers used for the HR construct: 5'-CACCGATGATCTGTTTTAAAATGTG-3' and 5'-AAACCACATTTTAAAACAGATC

ATC-3'. Co-transfection of ssDNA oligo and CRISPR plasmid (pX459) into K562 cells was performed by electroporation using Lonza SF cell line kit. Primers used for genotyping: forward primer: 5'-TAAGCAGAATTCATGCCACTTATTTGGGCAAT-3' and reverse primer: 5'-TGCTTAAAGCTTTGCCCATGAGATGGTCACTA-3'.

DNA damage assessed by Western blot and CFGE

After 2-hour drug treatment of indicated drugs at 5μM, cells were washed with PBS. WB and CFGE were performed as described [11]. Images were quantified with ImageJ.

Fractionation assay

Endogenously tagged GFP-H2B cells (1×10^6) were pre-incubated with protease inhibitor cocktail (P1860-1ML, Sigma-Aldrich) for 1 hour followed by 3-hour treatment with 10 μM of the indicated drugs. Cells were dissolved in lysis buffer (50mM Tris-HCl pH 8.0, 150 mM NaCl, 5 mM $MgCl_2$, 0.5% NP40, 2.5% glycerol supplemented with protease inhibitors, 10 mM NMM) for 5 min on ice, and then centrifuged for 10 min at 15,000 g at 4°C. Both nucleus (pellet) and cytosol (supernatant) were washed once and submitted for Western Blot analysis. Primary antibodies used for detection: GFP (1:1000) [12], Lamin B1 (1:1000, 12987-I-AP, Proteintech), Calnexin (1:1000, C5C9, Cell signaling).

Time-lapse confocal microscopy

For time-lapse confocal imaging, MelJuSo cells were seeded in 35-mm bottom petri dish (Poly-dlysin Coated, MatTek Corporation), transfected with TopoIIα-GFP construct (effectene, Qiagen) and imaged upon treatment with the indicated drugs [2]. Leica SP8 confocal microscope system, 63×lens, equipped with a climate chamber was used. TopoIIα-GFP distribution was quantified using Leica Application Suite X software.

Short-term cell viability assay

Twenty-four hours after seeding into 96-well plates, cells were treated with indicated drugs for 2 hours at physiologically relevant concentrations [2]. Subsequently, drugs were removed by extensive washing, and cells were cultured for an additional 72 hours. Cell viability was measured using the CellTiter-Blue viability assay (Promega). Survival was normalized to the untreated control samples after correction for the background signal.

ChIP-seq

Endogenous tagged 3×Flag-TopoIIα K562 cells were treated with 10 μM of indicated drugs for 4 hours. Cells were fixed and processed as described [3, 13]. ChIP was done with anti-Flag M2 (F3165, Sigma), followed by sequencing on an Illumina Hiseq2000 platform (Genome Sequencing Service Center of Stanford Center for Genomics and Personalized Medicine Sequencing Center).

ChIP-seq data were processed identically using the ENCODE Data Coordination Center (DCC) ChIP-seq pipeline (https://github.com/ENCODE-DCC/chip-seq-pipeline2) (v1.9.0). Briefly, the ChIP-seq reads were aligned to the human reference genome (GRCh37/hg19) using Bowtie2 [14]. Duplicate reads were removed using Picard MarkDuplicates (RRID:SCR_006525). Peaks of each sample were called against the whole-cell lysates replicates using SPP [15] with the parameters '-npeak 300000 -speak 155 -fdr 0.01'. The

blacklisted regions described by ENCODE were discarded [16]. Reproducible peaks were intersected from two biological replicates and annotated with epigenomic signatures of K562, downloaded from the Roadmap Epigenomics Project [17]. Normalized TopoIIα binding affinity matrix: consensus peaks by samples, principle component analysis and differential binding affinity analysis were performed using the R package DiffBind [18].

ATAC-seq

K562 cells were treated with 10 μM of indicated drugs for 4 hours. Cells were fixed and processed as described [19, 20]. DNA was processed using a customized library preparation method for ATAC-seq and was sequenced using an Illumina HiSeq4000 platform.

ATAC-seq data were processed identically using the ENCODE Data Coordination Center (DCC) ATAC-seq pipeline (https://github.com/ENCODE-DCC/atac-seq-pipeline) (v1.10.0). Briefly, the ATAC-seq reads were aligned to the human reference genome (GRCh37/hg19) using Bowtie2 [14]. Duplicate reads were removed using Picard MarkDuplicates (RRID:SCR_006525). Peaks were called using MACS2 [21] with the setting of '-p 0.01 --shift -75 --extsize 150 --nomodel -B --SPMR --keep-dup all', then followed by blacklisted regions filtering described by ENCODE [16]. Reproducible peaks were identified from two biological replicates and annotated with epigenomic signatures of K562, downloaded from the Roadmap Epigenomics Project [17]. ATAC-seq signal tracks for all the samples were generated by bedtools with the command 'bedtools genomecov -scale' using the read count per million (CPM) normalization and convert to bigwig files using bedGraphToBigWig. Normalized ATAC-seq read density matrix: consensus peaks by samples, principle component analysis and differential chromatin accessibility analysis were performed using the R package DiffBind [18].

The bio-distribution of anthracyclines in mice

FVB/NRj mice ordered from Janvier Labs (Le Genest-Saint-Isle, France) were housed in individually ventilated cages under specific pathogen-free conditions in the animal facility of the NKI (Amsterdam, The Netherlands). All mouse experiments were approved by the Animal Ethics Committee of the NKI and were performed according to institutional and national guidelines. Male mice (8-week old) were i.v. injected with Doxo, Acla, Amr, Epi or Ida at 5 mg/kg (n = 5 per group). Four hours post injection, animals were sacrificed, and plasma, heart, lung, liver, kidney, spleen, brain, thymus, axillary and inguinal lymph nodes, and testis+epididymis were collected. Hearts were cut into two pieces with coronal section. One piece was fixed in EAF fixative (ethanol/acetic acid/formaldehyde/saline, 40:5:10:45 v/v/v/v) and processed for Phospho-H2AX (Ser139) IHC (1:100, #2577, Cell Signaling). The other half of the heart and the rest of organs were weighted, frozen and analyzed by LC-MS/MS [5].

The cardiotoxicity of anthracyclines in mice

FVB/NRj mice (10–11-week old) were i.v. injected with 5 mg/kg of Doxo, 5 mg/kg of Acla, or 5 ml/kg of saline every 2 weeks for 4 times. After 4-week interval, the animals were i.v. injected with 5 mg/kg of indicated drug or 5 ml/kg of saline every 2 weeks for another 4 times. The mice were monitored every other day. When body weight loss was more than 20%, or circulation failure occurred, animal was euthanized by CO_2. Subsequently, full body anatomy was performed. All organs were collected, fixed in EAF fixative and embedded in paraffin. Sections were cut at 2 μm from the paraffin blocks and stained with hematoxylin and eosin, and 4 μm for immunohistochemistry of Desmin (1:200, M0760, DakoCytomation), Vimentin (1:100, #5741, Cell Signaling), or Periostin (1:100, ab215199, Abcam). Pathology slides were reviewed twice by an expert mouse pathologist who was

blind to the treatment. Incidence rate (IR = [number of mice with the specific side effect over a time period]/[sum of mice × time at risk during the same time period]) and cumulative incidence (CI = [number of mice with specific side effect at end time point]/[total number of mice at start]) were calculated for indicated side effects.

r/rAML patients

Patients with refractory or relapse AML treated between July 2012 and July 2022 at Ruijin hospital, China were enrolled in this retrospective study. Some patients participated in trail ChiCTR-OPC-14005712, ChiCTR-OPC-15006896, ChiCTR-IIR-16008809, ChiCTR-OIC-16008952, ChiCTR-IIR-16008962 and ChiCTR-IIR-17011677. This study was approved by the ethics committee of Ruijin Hospital, all patients provided written informed consent. Cytogenetic risk was classified according to the modified Southwest Oncology Group criteria [22], and integrated risk was classified as described [23]. The treatment details were decribed in supplemental materials and methods. The baseline characteristics and clinical outcomes of the patients are summarized in supplemental Tables 1 and 2, respectively.

Cytogenetic risk was classified according to the modified Southwest Oncology Group criteria [22]: (1) favorable risk, including t(8;21) and inv(16) or t(16;16)(p13;q22); (2) unfavorable risk, including del(5q) or monosomy 5, monosomy 7 or del(7q), abnormal 3q, 9q, 11q, 21q, or 17p, t(6;9), t(9;22), and complex karyotypes (three or more unrelated chromosomes abnormal); and (3) intermediate risk, including normal karyotypes and all other anomalies. FLT3 internal tandem duplication and mutations in CEBPA, NPM1 and IDH1/2 were tested. Integrated risk was classified as described [23]. CR was defined as bone marrow blasts <5%, absolute neutrophil count $\geq 1\times10^9$/L, and platelet count $\geq 100\times10^9$/L, and absence of extramedullary disease. Partial remission was defined as having <15% (and a 50% decrease in bone marrow blasts) but >5% blasts or with <5% blasts but not reaching the CR

220 criteria for blood cell count or clinical manifestation. The baseline characteristics and clinical
221 outcomes of the patients are summarized in supplemental Tables 1 and 2, respectively.
222
223 ## AML treatments
224 CAG patients were treated with 15□25 mg/m^2 of Ara-C (cytarabine) injected s.c. every 12 h
225 on days 1□14, 20 mg/d of Acla infused i.v. on days 1□4, and 200 μg/m^2 of granulocyte
226 stimulating factor (G-CSF) administered s.c. daily on days 1□14. G-CSF was reduced, or
227 temporarily stopped when neutrophilia was >5×10^9/L. IA patients were treated with 6□10
228 mg/m^2 of Ida infused i.v. on days 1□3 and 100□200 mg/m^2 of Ara-C on days 1□7. VA
229 patients were injected with 75 mg/m^2 of azacitidine s.c. daily on days 1□7, and administered
230 with venetoclax orally, once daily. The dose of venetoclax was 100 mg on day 1 and 200 mg
231 on day 2; and 400 mg on days 3□28. In all subsequent 28-day cycles, the dose of venetoclax
232 was initiated at 400 mg daily. The other induction chemotherapy for r/rAML patients
233 included IA, DA, FLAG, CLAAG and CHA regimens. For patients treated with DA regimen,
234 20 mg/m^2 of decitabine was administered i.v. daily on days 1□5, and 1 g/m^2 of Ara-C was
235 injected every 12 hours on days 6□7. For patients treated with FLAG regimen, fludarabine
236 was infused i.v. at 30 mg/m^2 on days 2□6; 4 hours after fludarabine infusion, Ara-C was
237 injected i.v. at 1.5□2 g/m^2 over 3 hours on days 2□6; G-CSF was administered at 5 μg/kg s.c.
238 on days 1□5; additional G-CSF may be administered since 7 days after the end of
239 chemotherapy until WBC count >500/uL. For patients >60-year-old, the dose may be reduced
240 to 20 mg/m^2 for fludarabine and 0.5□1 g/m^2 for cytarabine. For patients treated with CLAAG
241 regimen, 5 mg/m^2 of cladribine was infused i.v. over 2 hours on days 1□5; 15 mg/m^2 of Ara-
242 C was injected s.c. every 12 hours on days 1□10; trans retinoic acid (ATRA) was
243 administered orally at 45 mg/m^2 on days 4□6, then at 15 mg/m^2 on days 7□20; 300 μg G-
244 CSF was injected s.c. on day 0. For patients treated with CHA regimen, 5 mg/m^2 of

cladribine was infused i.v. over 2 hours on days 1□5; 2 mg/m^2 of homoharringtonine was infused i.v. over 2 hours on days 1□5; 1 g/m^2 of Ara-C was injected 2 hours after cladribine on days 1□5.

Statistical analyses

Results are shown as mean ± SEM or mean ± SD. Statistical analysis was performed using Prism unless otherwise specified. All the in vitro experiments were performed with a minimum of three independent trials with the exception of ChIP-seq and ATAC-seq which were in biological duplicates. All the animals of mouse experiments are shown in the dot plots. Statistical tests are indicated in each figure legend.

Results

Mechanisms of action and cross-resistance of anthracyclines

To assess whether the various clinically administered anthracyclines (Fig. 1A) differ in their DNA- and chromatin-damaging activities, as well as cross-resistance, we exposed AML cell line THP1 at a clinically relevant dose for 2 hours followed by further culturing to mimic the pharmacokinetics in patients [24]. DNA damage was assessed by constant-field gel electrophoresis (CFGE) [11] and phosphorylation of H2AX at Ser139 (γH2AX) [25] as detected by Western blotting. Doxorubicin (Doxo), daunorubicin (Daun), epirubicin (Epi), idarubicin (Ida), and amrubicin (Amr) all induced DSBs, unlike aclarubicin (Acla) (Fig. 1B–E). Next, chromatin damage as the result of histone eviction was visualized by a fractionation assay using K562 cells with endogenously tagged GFP-H2B. Except for Amr, all the tested anthracyclines induced histone release from nucleus and accumulation in cytosol (Fig. 1F,G; Fig. S1A). Furthermore, all histone-evicting anthracyclines were able to redistribute GFP-TopoIIα on chromatin (Fig. S1B,C). Cytotoxicity assays revealed poor anti-cancer activity

for the DNA-damaging analog Amr, while the other analogs bearing chromatin-damaging activity were effective in eliminating various myeloid leukemia cell lines (Fig. 1H).

In addition to treatment-limiting cardiotoxicity, drug resistance could also limit the effect of anthracycline drugs. ABCB1 is a major drug efflux transporter contributing to anthracycline resistance [26]. We generated a Doxo-resistant leukemia cell line by overexpressing ABCB1 [10] and tested its sensitivity to other anthracyclines (Fig. 1I–K; Fig. S1D). The ABCB1-overexpressing cells acquired resistance to Doxo, Daun, Epi and Amr, but failed to export Ida and Acla efficiently (Fig. 1J,K). These data together indicate that clinically relevant anthracyclines should be considered as distinct drugs with unique features and different efficiencies. Evicting histones and relocalizing TopoIIα while not inducing DSBs, as in the case of Acla, apparently suffices for efficient cytotoxicity.

Epigenetic selectivity of TopoIIα redistribution and histone eviction of anthracyclines

Anthracyclines poison TopoII by disrupting its interface with DNA by their sugar moieties and the cyclohexene ring [27]. However, the anthracycline-specific redistribution of TopoII and its association with histone eviction have not been characterized. We addressed this in K562 cells whose epigenomic information has been extensively profiled by ENCODE consortium [28]. Chromatin immunoprecipitation followed by deep sequencing (ChIP-seq) against endogenously tagged TopoIIα was performed 4 hours after anthracycline exposure in independent duplicate experiments (Fig. S2A). The resulting ChIP-seq profiles analyzed by principal component analysis (PCA) suggested that all histone-evicting anthracyclines cause extensive and drug-specific TopoIIα redistribution as compared to untreated or Amr-treated cells (Fig. 2A,B). To characterize this drug-specific TopoIIα redistribution, we coupled the ChIP-seq data to the epigenetic information of ENCODE (Fig. 2C). With the same sugar

295 moiety and cyclohexane (Fig. 1A), Daun and Doxo (also labeled as hydroxyDaun) depleted
296 TopoIIα from active chromatin regions, like DNase I hypersensitive regions (DHS),
297 H3K4me1, H3K4me2, H3K4me3, H3K9ac, H3K27ac, H3K79me2 and H2A.Z [29]. Instead,
298 TopoIIα was trapped in compact chromatin regions marked by H3K27me3 [29], H3K9me1
299 [30] and H3K9me3 [31] (Fig. 2C). Ida and Acla depleted TopoIIα from broader chromatin
300 states, except for H3K9me3 [31], H3K27me3 [29] and H3K36me3 [31] decorated regions
301 (Fig. 2C). Epi, with an epimerizing hydroxyl group at the sugar moiety (Fig. 1A), further
302 depleted TopoIIα from H3K36me3 [31] modified regions (Fig. 2C). It is worth noting that the
303 redistribution of TopoIIα at regions with unknown epigenetic features was increased for all
304 drugs, except for Amr (Fig. 2C).

305 While the TopoIIα redistribution showed drug specificity, we continued to identify
306 histone eviction preferences of each anthracycline using transposase-accessible chromatin
307 with sequencing (ATAC-seq) [19] in K562 cells (Fig. 2D). In line with its lack of chromatin-
308 damaging activity (Fig. 1F,G), Amr failed to induce *de novo* open chromatin and could
309 therefore be found close to untreated cells in PCA plot (Fig. 2E). Similar to the TopoIIα
310 redistribution pattern, the other tested anthracyclines evicted histones mostly from open
311 chromatin regions, once again exhibiting distinct preferences (Fig. 2F). As histone
312 modifications are required for recruitment of TopoIIα to DNA [32], selective eviction of
313 histones from open chromatin regions may contribute to the observed depletion of TopoIIα
314 from the same regions. Based on the comparative analysis of TopoIIα ChIP-seq and the
315 ATAC-seq experiments, we observed that regions identified by both ATAC-seq and TopoIIα
316 ChIP-seq were greatly decreased by histone-evicting anthracyclines (Fig. 2G,H; Fig. S2B).
317 Nonetheless, outside of overlapping regions, TopoIIα redistribution and *de novo* accessible
318 chromatin were usually not associated with each other, indicating that these may constitute
319 two independent effects of anthracyclines (Fig. S2B). Thus, integration of TopoIIα ChIP-seq

and ATAC-seq revealed the connection between histone eviction and TopoIIα depletion in transcriptionally active regions, as well as selective impact of each analog on the epigenetic landscape. Each clinically used anthracycline has individual genomic preferences, which may define drugs with different specificity.

Bio-distribution of anthracyclines

Acla is effective in eliminating a large variety of cancer cells in tissue culture [5]. However, it is mainly used in treating AML and is less effective against solid tumors [33, 34]. This could be the result of differences in biodistribution of anthracyclines. To test this, we performed a comprehensive pharmacokinetic study for Acla and the other clinically used anthracyclines in mice. Four hours post iv injection of a clinically relevant dose of indicated drug at 5 mg/kg [35], Doxo, Epi and Ida showed similar bio-distribution patterns across different organs (Fig. 3A; Fig. S3A). Amr had a similar tissue distribution as Doxo, but showed reduced distribution to lung, kidneys, and heart. Brain tissue was poorly penetrated by all drugs (Fig. 3A; Fig. S3A). A notable exception was Acla, which accumulated in lymphoid organs (spleen, thymus and lymph nodes) but poorly distributed to other organs (Fig. 3A; Fig. S3A). This might be an explanation why Acla is ineffective in treating solid tumors, as opposed to hematologic tumors.

We further evaluated DNA damage in the heart in response to drug exposure. While Doxo, Epi and Ida incited persistent DNA damage in the heart, the hearts of Acla- and Amr-treated mice did not show any γH2AX signals 4 hours after drug administration (Fig. 3B; Fig. S3B), in line with poor tissue penetration of Acla and Amr and the fact that Acla does not induce DNA damage at all.

Acla is safe and well tolerated following Doxo treatment

Doxo, Daun, Ida and Epi all induce cumulative dose-dependent cardiotoxicity, which limits patient treatment to only few courses. Since Acla treatment is not associated with cardiotoxicity [5], we reasoned that it could be safe to apply this drug to mice following treatment with cardiotoxic anthracyclines. To test this, Acla was administered to mice after half-maximum cumulative dose of Doxo (Fig. 4A) and followed over time. Cardiotoxicity induced by Doxo caused cardiac hypertrophy and remodeling that presented as thrombus formation in the left atrium and auricle of the heart accompanied by inflammation, fibrosis and calcification [5, 36] (Fig. 4B; Fig. S4A). Further staining for profibrotic proteins vimentin [37] and periostin [38], and cytoskeletal protein desmin [39], revealed impairment of myocytes and fibrosis in the stroma (Fig. 4C–H; Fig. S4B–F). With impaired cardiac function, Doxo-treated mice died from circulation failure (Fig. 4I).

Reflecting clinical observations [40] and our prior work [5], the incidence, latency and histopathological alterations of Doxo-induced cardiotoxicity developed in a dose-dependent manner (Fig. 4A, D-C vs D-D), whereas eight courses of Acla treatment showed no abnormalities in the heart (Fig. 4F–K; Fig. S4, A-A vs C-C/D-C/D-D). More importantly, Acla treatment after half-maximum cumulative dose of Doxo did not aggravate cardiotoxicity (Fig. 4; Fig. S4, D-A vs D-D). Similarly, pre-treatment with Acla did not make mice more susceptible to Doxo-induced cardiotoxicity (Fig. 4; Fig. S4, A-D vs D-C/D-D). Hence, Acla is safe and well tolerated following Doxo treatment in this model system. Considering limited cardiotoxicity, little cross-resistance and differences in epigenomic specificities between anthracyclines, Acla would be predicted to act as an independent drug in salvage relapsed/refractory AML (r/rAML) patients who have already received the maximum cumulative dose of cardiotoxic anthracyclines. Such systematic studies have not been reported.

CAG strongly improves the survival of relapsed/refractory AML patients

R/rAML is one of the most challenging situations in hematology, with a 5-year overall survival (OS) of only 10% [41]. The prognosis of elderly or unfit r/rAML patients is even more disappointing [42]. Unfortunately, no specific salvage regimen has appeared as a standard treatment for r/rAML [42]. CAG regimen, containing low-dose of cytarabine, Acla and G-CSF, has been widely used in China and Japan for treating AML [43, 44]. It is well tolerated by r/r and elderly AML patients with lower toxicity than conventional chemotherapies [43-45]. To compare the efficacy of CAG to other salvage chemotherapies in r/rAML, we conducted a single-center retrospective study at Ruijin hospital (Shanghai, China).

A total of 186 r/rAML patients, treated between July 2012 and July 2022, were included in the study. In this group of patients, fit patients with *de novo* AML often received Ida in combination with cytarabine (IA) rather than Daun or Doxo for first-line therapy, as Ida is more effective for induction therapy in AML [46, 47]. However, all three anthracyclines are cardiotoxic [48]. Among the patients who developed refractory and relapse after primary IA treatment for *de novo* disease, 66 patients received CAG regimen (2^{nd}-line CAG group), 67 received other chemotherapy regimens (2^{nd}-line others group), and 34 received emerging target therapy regimen venetoclax + azacitidine (2^{nd}-line VA group) (Fig. 5A). 19 patients who were treated with CAG for both *de novo* and r/r diseases were enrolled to illustrate that Acla does not contribute to cardiotoxicity and is compatible with extended treatment (1^{st}&2^{nd}-line CAG group) (Fig. 5A). Notably, at Ruijin hospital, CAG is usually applied to *de novo* AML patients with unfit conditions who are not expected to tolerate conventional intensive chemotherapies. The demographic and clinical characteristics of all patients at r/rAML diagnosis are summarized in supplemental Table 1. There was no significant difference between 2^{nd}-line CAG group and any other group with respect to age, gender,

French-American-British type, cytogenetic risk, and frequent oncogenic mutations. Slightly more patients in the 2nd-line others group were diagnosed with favorable integrated risk than in the other arms of the study.

The overall complete remission (CR) rate after induction was 74% for the 2nd-line CAG group, which is significantly higher than that of the 2nd-line others (37%) and the 2nd-line VA group (35%) (Table 1). Patients with favorable and intermediate cytogenetics or integrated risk responded better to CAG. However, cytogenetics or integrated risk was not prognostic for the other groups (Table 1). Among the patients with a favorable and intermediate risk, the complete remission rate of 2nd-line CAG was superior to that of 2nd-line others and the 2nd-line VA group (Table 1). While age is a poor prognostic factor for AML [42], no significant difference was seen for CAG outcome in patients <60- and ≥60-year-old. Actually, for patients ≥60-year-old, 2nd-line CAG also outperformed other treatment regimens (Table S2). No CR and major prognostic mutation associations were detected for any treatment group due to small cohort (Table S2). In terms of CR rate, compared to the 2nd-line CAG group that first received IA, the 1st&2nd-line CAG group performed slightly less optimally due to unfit conditions. However, this treatment protocol was not inferior to the 2nd-line others and the 2nd-line VA group (Table 1; Table S2), suggesting that CAG remains effective and tolerable in unfit r/rAML patients, even after prior CAG treatments.

Since both CAG and VA therapy were well tolerated, some patients continued with these regimens for consolidation therapy and long-term maintenance. Among these were patients treated for up to 11 times with CAG without any cardiac issues, far more than other anthracyclines (Fig. S5A). This strategy was not an option for IA treatment due to accumulated cardiotoxicity and resistance. Superior CR rates and/or sustainable treatment schedule of CAG and VA translated into a more than 20% better OS as compared to 2nd-line others group (Fig. 5B,C; Fig. S5B,C). Nonetheless, event-free survival analysis indicated a

better durable response of 2nd-line CAG when compared to 2nd-line VA (Fig. 5D,E), possibly due to the development of VA resistance [49]. Of note, the 1st&2nd-line CAG patients were selected for the limited toxicity of this regimen due to unfit conditions, which is associated with poor prognosis. Still, these patients achieved comparable OS as the 2nd-line CAG group (Fig. 5B,C; Fig. S5D,E). Taken together, these findings reveal that CAG regimen can be a superior, low-toxicity chemotherapy for r/rAML, including those with unfit conditions.

Discussion

Despite their devastating side effect profiles, anthracyclines including doxorubicin, daunorubicin and idarubicin have been cornerstones of oncology treatment for over 50 years. While the molecular mechanisms of action have been mostly considered the same across different anthracycline analogs, clinical observations and our previous studies have indicated that this does not apply to all variants [2, 3, 5, 50]. Here, we performed a comprehensive analysis of clinically relevant anthracyclines against key parameters including mode of action, epigenomic selectivity and clinical performance, and find individual anthracyclines have substantially different pharmacological properties. In the course of our evaluation, Acla stood out as it is minimally cardiotoxic and prefers lymphoid organs over solid tissues. Attributing to its high therapeutic index for AML, we demonstrate that Acla can be safely used in second-line therapy after initial treatment of cardiotoxic anthracyclines, leading to 23% higher 5-year OS for r/rAML patients.

A common feature of anthracyclines is their poisoning of TopoIIα. TopoIIα plays a role in all areas of chromosome structure, from nucleosome assembly and disassembly to chromosome condensation and segregation between daughter cells [51-53]. DSB induction mediated by the catalytic activity of TopoIIα has always been considered as the primary cytotoxic mechanism of anthracyclines [1]. However, this dogma is challenged by Acla and

445 other anthracycline variants whose major cytotoxic activity is chromatin damage, also known
446 as histone eviction [54]. It has been reported that deregulation of TopoIIα leads to cell death
447 in a manner independent of its catalytic activity [55, 56]. Therefore, without poisoning
448 TopoIIα for DNA damage, depleting and redistributing TopoIIα are already detrimental, as
449 illustrated by Acla. This finding further uncovers the anti-cancer mechanism of chromatin
450 damage caused by histone eviction.

451 While Acla was first introduced into clinic 40 years ago (it was available in Europe until
452 2004 and was never registered in the U.S.), it is surprising that the unique effects of Acla in
453 r/rAML has never been realized. Our data suggest that applying CAG therapy in r/rAML
454 patients would increase their 5-year OS by 23%. If Acla was incorporated into current AML
455 regimens, 10,000 r/rAML patients in the U.S. and Europe [57] would survive annually from
456 this off-patent and low-cost drug. The impact on pediatric oncology will be even more
457 profound, as 50% of childhood cancer patients receive high-dose anthracyclines and go on to
458 have 5- to 15-fold increased risk for heart failure compared to the general population [9].
459 Introducing Acla in their treatment would mitigate this side effect. Considering old drugs in
460 new ways may therefore substantially – and expeditiously – improve the survival and quality
461 of life of many cancer patients, as exemplified here.

462

463 # Abbreviations

Acla	Aclarubicin
AML	Acute myeloid leukemia
Amr	Amrubicin
Ara-C	Cytarabine
ATAC-seq	Assay for Transposase-Accessible Chromatin using sequencing
ATRA	Retinoic acid
CAG	cytarabine, Acla and G-CSF
CFGE	Constant-field gel electrophoresis
ChIP-seq	Chromatin immunoprecipitation followed by sequencing

CR	Complete remission
Daun	Daunorubicin
DHS	DNase I hypersensitive regions
Doxo	Doxorubicin
DSBs	DNA double-strand breaks
Epi	Epirubicin
FCS	Fetal calf serum
G-CSF	Granulocyte colony stimulating factor
GEO	Gene expression omnibus
IA	Ida in combination with cytarabine
Ida	Idarubicin
IMDM	Iscove's modified dulbecco's medium
IR	Incidence rate
OS	Overall survival
PCA	Principal component analysis
γH2AX	phosphorylation of H2AX at Ser139
r/rAML	relapsed/refractory AML
SDS	Sodium dodecyl sulfate
TopoII	Topoisomerase II

Supplementary Information

Supplementary Materials.dox includes Figures S1 to S5 and Tables S1 to S2.

Declarations

Ethics approval and consent to participate

All mouse experiments were approved by the Animal Ethics Committee of the NKI and were performed according to institutional and national guidelines. The retrospective clinical study was approved by the ethics committee of Ruijin Hospital, and all patients provided written informed consent.

Availability of data and materials

The sequencing data supporting the findings of this study are available at the Gene Expression Omnibus (GEO) under accession numbers GSE240443 (https://www.ncbi.nlm.nih.gov/geo/query/acc.cgi?acc=GSE240443). Source data are provided with this paper. Clinical data are available from the corresponding authors upon reasonable request and with permission of Ruijin hospital.

Competing interests

J.N. is a shareholder in NIHM that aims to produce Acla for clinical use. The authors do not declare any other competing interests.

Funding

This work was supported by grants from the European Research Council (ERC) (advanced grant ERCOPE 694307) (J.N.), Dutch Cancer Society (KWF 11356) (J.N.), Institute for Chemical Immunology from NWO Gravitation (NWO 024.002.009) (J.N.), Spinoza award funded by the Ministry of Education, Culture and Science of the Netherlands (NWO 00897590) (J.N.), RIKI foundation (C.L.Z.).

Authors' contribution

Contribution: X.Q., S.Y.v.d.Z. and J.N. designed experiments. X.Q. and S.Y.v.d.Z. performed experiments. O.v.T., F.L.H., and M.A.v.G. contributed to experiments. Y.Z. and X.L. collected the r/rAML data. X.Q., X.L., J.L. and J.N. analyzed the clinical data. M.T. and B.P. performed and analyzed ChIP-seq and ATAC-seq experiments. L.J., Y.L. and B.P. made stable cell lines. J.S. performed pathological analyses. C.L.Z. contributed to the result interpretation. X.Q., S.Y.v.d.Z. and J.N. wrote the manuscript, with the input of all authors. All authors read and approved the final manuscript.

Acknowledgements

The authors thank the people from the Preclinical Intervention Unit of the Mouse Clinic for Cancer and Ageing (MCCA) at NKI for their technical support performing the animal experiments and the staff from the Experimental Animal Pathology facility at NKI for their service on histochemistry and immunochemistry staining; Prof. J.P. Vandenbroucke and M. Schaapveld for help with the epidemiological assessment of clinical data; J. Sarthy and I. Berlin for comments and critical reading of the Manuscript.

References

1. Tewey KM, Rowe TC, Yang L, Halligan BD, Liu LF. Adriamycin-induced DNA damage mediated by mammalian DNA topoisomerase II. Science. 1984;226(4673):466-8.
2. Pang B, Qiao X, Janssen L, Velds A, Groothuis T, Kerkhoven R, et al. Drug-induced histone eviction from open chromatin contributes to the chemotherapeutic effects of doxorubicin. Nature communications. 2013;4:1908.
3. Pang B, de Jong J, Qiao X, Wessels LF, Neefjes J. Chemical profiling of the genome with anti-cancer drugs defines target specificities. Nature chemical biology. 2015;11(7):472-80.
4. Yang F, Kemp CJ, Henikoff S. Doxorubicin enhances nucleosome turnover around promoters. Curr Biol. 2013;23(9):782-7.
5. Qiao X, van der Zanden SY, Wander DPA, Borras DM, Song JY, Li X, et al. Uncoupling DNA damage from chromatin damage to detoxify doxorubicin. Proceedings of the National Academy of Sciences of the United States of America. 2020;117(26):15182-92.
6. Girling DJ. Comparison of oral etoposide and standard intravenous multidrug chemotherapy for small-cell lung cancer: a stopped multicentre randomised trial. Medical Research Council Lung Cancer Working Party. Lancet. 1996;348(9027):563-6.
7. Hong WK, Nicaise C, Lawson R, Maroun JA, Comis R, Speer J, et al. Etoposide combined with cyclophosphamide plus vincristine compared with doxorubicin plus cyclophosphamide plus vincristine and with high-dose cyclophosphamide plus vincristine in the treatment of small-cell carcinoma of the lung: a randomized trial of the Bristol Lung Cancer Study Group. Journal of Clinical Oncology. 1989;7(4):450-6.
8. Sekeres MA, Guyatt G, Abel G, Alibhai S, Altman JK, Buckstein R, et al. American Society of Hematology 2020 guidelines for treating newly diagnosed acute myeloid leukemia in older adults. Blood Adv. 2020;4(15):3528-49.

9. Armenian S, Bhatia S. Predicting and Preventing Anthracycline-Related Cardiotoxicity. Am Soc Clin Oncol Educ Book. 2018;38:3-12.
10. Li Y, Tan M, Sun S, Stea E, Pang B. Targeted CRISPR activation and knockout screenings identify novel doxorubicin transporters. Cell Oncol (Dordr). 2023.
11. Wlodek D, Banath J, Olive PL. Comparison between pulsed-field and constant-field gel electrophoresis for measurement of DNA double-strand breaks in irradiated Chinese hamster ovary cells. International journal of radiation biology. 1991;60(5):779-90.
12. van der Kant R, Fish A, Janssen L, Janssen H, Krom S, Ho N, et al. Late endosomal transport and tethering are coupled processes controlled by RILP and the cholesterol sensor ORP1L. J Cell Sci. 2013;126(Pt 15):3462-74.
13. Schmidt D, Wilson MD, Spyrou C, Brown GD, Hadfield J, Odom DT. ChIP-seq: using high-throughput sequencing to discover protein-DNA interactions. Methods. 2009;48(3):240-8.
14. Langmead B, Salzberg SL. Fast gapped-read alignment with Bowtie 2. Nat Methods. 2012;9(4):357-9.
15. Kharchenko PV, Tolstorukov MY, Park PJ. Design and analysis of ChIP-seq experiments for DNA-binding proteins. Nat Biotechnol. 2008;26(12):1351-9.
16. Amemiya HM, Kundaje A, Boyle AP. The ENCODE Blacklist: Identification of Problematic Regions of the Genome. Scientific reports. 2019;9(1):9354.
17. Roadmap Epigenomics C, Kundaje A, Meuleman W, Ernst J, Bilenky M, Yen A, et al. Integrative analysis of 111 reference human epigenomes. Nature. 2015;518(7539):317-30.
18. Ross-Innes CS, Stark R, Teschendorff AE, Holmes KA, Ali HR, Dunning MJ, et al. Differential oestrogen receptor binding is associated with clinical outcome in breast cancer. Nature. 2012;481(7381):389-93.
19. Buenrostro JD, Giresi PG, Zaba LC, Chang HY, Greenleaf WJ. Transposition of native chromatin for fast and sensitive epigenomic profiling of open chromatin, DNA-binding proteins and nucleosome position. Nat Methods. 2013;10(12):1213-8.
20. Corces MR, Trevino AE, Hamilton EG, Greenside PG, Sinnott-Armstrong NA, Vesuna S, et al. An improved ATAC-seq protocol reduces background and enables interrogation of frozen tissues. Nat Methods. 2017;14(10):959-62.
21. Zhang Y, Liu T, Meyer CA, Eeckhoute J, Johnson DS, Bernstein BE, et al. Model-based analysis of ChIP-Seq (MACS). Genome biology. 2008;9(9):R137.
22. Slovak ML, Kopecky KJ, Cassileth PA, Harrington DH, Theil KS, Mohamed A, et al. Karyotypic analysis predicts outcome of preremission and postremission therapy in adult acute myeloid leukemia: a Southwest Oncology Group/Eastern Cooperative Oncology Group Study. Blood. 2000;96(13):4075-83.
23. Dohner H, Estey EH, Amadori S, Appelbaum FR, Buchner T, Burnett AK, et al. Diagnosis and management of acute myeloid leukemia in adults: recommendations from an international expert panel, on behalf of the European LeukemiaNet. Blood. 2010;115(3):453-74.
24. Greene RF, Collins JM, Jenkins JF, Speyer JL, Myers CE. Plasma pharmacokinetics of adriamycin and adriamycinol: implications for the design of in vitro experiments and treatment protocols. Cancer research. 1983;43(7):3417-21.
25. Kuo LJ, Yang LX. Gamma-H2AX - a novel biomarker for DNA double-strand breaks. In vivo. 2008;22(3):305-9.

26. Cox J, Weinman S. Mechanisms of doxorubicin resistance in hepatocellular carcinoma. Hepat Oncol. 2016;3(1):57-9.
27. Wang AH, Ughetto G, Quigley GJ, Rich A. Interactions between an anthracycline antibiotic and DNA: molecular structure of daunomycin complexed to d(CpGpTpApCpG) at 1.2-A resolution. Biochemistry. 1987;26(4):1152-63.
28. Gerstein MB, Kundaje A, Hariharan M, Landt SG, Yan KK, Cheng C, et al. Architecture of the human regulatory network derived from ENCODE data. Nature. 2012;489(7414):91-100.
29. Barski A, Cuddapah S, Cui K, Roh TY, Schones DE, Wang Z, et al. High-resolution profiling of histone methylations in the human genome. Cell. 2007;129(4):823-37.
30. Alvarez F, Munoz F, Schilcher P, Imhof A, Almouzni G, Loyola A. Sequential establishment of marks on soluble histones H3 and H4. The Journal of biological chemistry. 2011;286(20):17714-21.
31. Rea S, Eisenhaber F, O'Carroll D, Strahl BD, Sun ZW, Schmid M, et al. Regulation of chromatin structure by site-specific histone H3 methyltransferases. Nature. 2000;406(6796):593-9.
32. Zhang M, Liang C, Chen Q, Yan H, Xu J, Zhao H, et al. Histone H2A phosphorylation recruits topoisomerase IIalpha to centromeres to safeguard genomic stability. EMBO J. 2020;39(3):e101863.
33. Kerpel-Fronius S, Gyergyay F, Hindy I, Decker A, Sawinsky I, Faller K, et al. Phase I-II trial of aclacinomycin A given in a four-consecutive-day schedule to patients with solid tumours. A South-East European Oncology Group (SEEOG) Study. Oncology. 1987;44(3):159-63.
34. Martino S, Decker DA, Hynes HE, Kresge CL. Phase II evaluation of aclacinomycin-A in advanced ovarian carcinoma. Investigational new drugs. 1987;5(4):373-4.
35. Johnson SA, Richardson DS. Anthracyclines in haematology: pharmacokinetics and clinical studies. Blood Rev. 1998;12(1):52-71.
36. Fujihira S, Yamamoto T, Matsumoto M, Yoshizawa K, Oishi Y, Fujii T, et al. The high incidence of atrial thrombosis in mice given doxorubicin. Toxicol Pathol. 1993;21(4):362-8.
37. Lencova-Popelova O, Jirkovsky E, Mazurova Y, Lenco J, Adamcova M, Simunek T, et al. Molecular remodeling of left and right ventricular myocardium in chronic anthracycline cardiotoxicity and post-treatment follow up. PloS one. 2014;9(5):e96055.
38. Zhao S, Wu H, Xia W, Chen X, Zhu S, Zhang S, et al. Periostin expression is upregulated and associated with myocardial fibrosis in human failing hearts. J Cardiol. 2014;63(5):373-8.
39. Guo R, Hua Y, Ren J, Bornfeldt KE, Nair S. Cardiomyocyte-specific disruption of Cathepsin K protects against doxorubicin-induced cardiotoxicity. Cell Death Dis. 2018;9(6):692.
40. Lotrionte M, Biondi-Zoccai G, Abbate A, Lanzetta G, D'Ascenzo F, Malavasi V, et al. Review and meta-analysis of incidence and clinical predictors of anthracycline cardiotoxicity. The American journal of cardiology. 2013;112(12):1980-4.
41. Ganzel C, Sun Z, Cripe LD, Fernandez HF, Douer D, Rowe JM, et al. Very poor long-term survival in past and more recent studies for relapsed AML patients: The ECOG-ACRIN experience. Am J Hematol. 2018;93(8):1074-81.
42. Dohner H, Estey E, Grimwade D, Amadori S, Appelbaum FR, Buchner T, et al. Diagnosis and management of AML in adults: 2017 ELN recommendations from an international expert panel. Blood. 2017;129(4):424-47.

613 43. Yamada K, Furusawa S, Saito K, Waga K, Koike T, Arimura H, et al. Concurrent use of granulocyte
614 colony-stimulating factor with low-dose cytosine arabinoside and aclarubicin for previously treated acute
615 myelogenous leukemia: a pilot study. Leukemia. 1995;9(1):10-4.
616 44. Wei G, Ni W, Chiao JW, Cai Z, Huang H, Liu D. A meta-analysis of CAG (cytarabine, aclarubicin, G-CSF)
617 regimen for the treatment of 1029 patients with acute myeloid leukemia and myelodysplastic syndrome.
618 Journal of hematology & oncology. 2011;4:46.
619 45. Jin J, Chen J, Suo S, Qian W, Meng H, Mai W, et al. Low-dose cytarabine, aclarubicin and granulocyte
620 colony-stimulating factor priming regimen versus idarubicin plus cytarabine regimen as induction therapy
621 for older patients with acute myeloid leukemia. Leuk Lymphoma. 2015;56(6):1691-7.
622 46. Owattanapanich W, Owattanapanich N, Kungwankiattichai S, Ungprasert P, Ruchutrakool T. Efficacy and
623 Toxicity of Idarubicin Versus High-dose Daunorubicin for Induction Chemotherapy in Adult Acute
624 Myeloid Leukemia: A Systematic Review and Meta-analysis. Clin Lymphoma Myeloma Leuk.
625 2018;18(12):814-21 e3.
626 47. Wang H, Xiao X, Xiao Q, Lu Y, Wu Y. The efficacy and safety of daunorubicin versus idarubicin
627 combined with cytarabine for induction therapy in acute myeloid leukemia: A meta-analysis of randomized
628 clinical trials. Medicine (Baltimore). 2020;99(24):e20094.
629 48. McGowan JV, Chung R, Maulik A, Piotrowska I, Walker JM, Yellon DM. Anthracycline Chemotherapy
630 and Cardiotoxicity. Cardiovasc Drugs Ther. 2017;31(1):63-75.
631 49. DiNardo CD, Tiong IS, Quaglieri A, MacRaild S, Loghavi S, Brown FC, et al. Molecular patterns of
632 response and treatment failure after frontline venetoclax combinations in older patients with AML. Blood.
633 2020;135(11):791-803.
634 50. Wu JF, Zhou JJ, Li XA, Hu LH, Wen ML. The safety and efficacy of amrubicin in the treatment of
635 previously untreated extensive-disease small-cell lung cancer: a meta-analysis. Onco Targets Ther.
636 2019;12:5135-42.
637 51. DiNardo S, Voelkel K, Sternglanz R. DNA topoisomerase II mutant of Saccharomyces cerevisiae:
638 topoisomerase II is required for segregation of daughter molecules at the termination of DNA replication.
639 Proceedings of the National Academy of Sciences of the United States of America. 1984;81(9):2616-20.
640 52. Uemura T, Yanagida M. Isolation of type I and II DNA topoisomerase mutants from fission yeast: single
641 and double mutants show different phenotypes in cell growth and chromatin organization. EMBO J.
642 1984;3(8):1737-44.
643 53. Uemura T, Ohkura H, Adachi Y, Morino K, Shiozaki K, Yanagida M. DNA topoisomerase II is required for
644 condensation and separation of mitotic chromosomes in S. pombe. Cell. 1987;50(6):917-25.
645 54. Wander DPA, van der Zanden SY, Vriends MBL, van Veen BC, Vlaming JGC, Bruyning T, et al. Synthetic
646 (N,N-Dimethyl)doxorubicin Glycosyl Diastereomers to Dissect Modes of Action of Anthracycline
647 Anticancer Drugs. The Journal of organic chemistry. 2021;86(8):5757-70.
648 55. Holm C, Goto T, Wang JC, Botstein D. DNA topoisomerase II is required at the time of mitosis in yeast.
649 Cell. 1985;41(2):553-63.
650 56. McPherson JP, Goldenberg GJ. Induction of apoptosis by deregulated expression of DNA topoisomerase
651 IIalpha. Cancer research. 1998;58(20):4519-24.

652 57. Seattle IfHMaEI, United States. Global Burden of Disease Study 2019 Results. Global Burden of Disease
653 Collaborative Network. 2020:Available from https://vizhub.healthdata.org/gbd-results/.

654

Clinical outcome	2nd-line CAG	2nd-line Others		2nd-line VA		1st&2nd-line CAG	
Complete remission	(n=65)	(n=51)	*P* value	(n=31)	*P* value	(n=17)	*P* value
Overall	48/65 (74%)	19/51 (37%)	0.0001†	11/31 (35%)	0.0006†	10/17 (59%)	0.2433†
Complete remission	0.0279‡		>0.9999‡		>0.9999‡		0.5500‡
Favourable and intermediate cytogenetics	40/50 (80%)	17/46 (37%)	<0.0001†	8/23 (35%)	0.0004†	8/13 (62%)	0.2704†
Unfavourable cytogenetics	5/11 (45%)	2/5 (40%)	>0.9999†	2/5 (40%)	>0.9999†	1/3 (33%)	>0.9999†
Unknown cytogenetics	3/4 (75%)	0/0 (NA)	>0.9999†	1/2 (50%)	>0.9999†	1/1 (100%)	>0.9999†
Complete remission	0.0087‡		>0.9999‡		0.2553‡		>0.9999‡
Favourable and intermediate integrated risk	34/40 (85%)	12/32 (38%)	<0.0001†	5/19 (26%)	<0.0001†	6/10 (60%)	0.0966†
Unfavourable integrated risk	9/18 (50%)	6/16 (38%)	0.7055†	6/12 (50%)	>0.9999†	3/5 (60%)	>0.9999†
Unknown integrated risk	5/7 (71%)	1/3 (33%)	0.5000†	0/0 (NA)	>0.9999†	1/2 (50%)	>0.9999†

Table 1. Treatment outcomes of r/rAML patients. CAG: cytarabin, aclarubicin, G-CSF; IA: idarubicin, cytarabine; VA: venetoclax, azacitidine; Others: chemotherapy regimens other than CAG. Data are n/N (%). † Fisher's exact test between the indicated group and 2nd-line CAG group. ‡ Fisher's exact test within group.

Figure 1. Acla differs from other anthracyclines in mechanisms of action and cross-resistance. (A) Structures of anthracyclines used in this study. Chemical moieties divergent from Doxo are depicted in red. (B) DNA damage examined by γH2AX Western blot. (C) Quantification of the γH2AX signal normalized to β-actin. Data are mean ± SEM; *n* = 4 biological replicates; Student's *t*-test. (D) DSBs analyzed by CFGE. (E) Quantification of relative broken DNA in (D). Data are mean ± SEM; *n* = 4 biological replicates; Student's *t*-test. (F) Histone eviction revealed by cell fractionation assay in K562-eGFP-H2B cells. N, nuclear fraction; C, cytosolic fraction. Calnexin and Lamin B1 are the loading control of each fraction. (G) The distribution of eGFP-H2B was quantified for both compartments. Data are mean ± SD; *n* = 4 biological replicates; two-way ANOVA. (H) IC_{50} of each anthracycline in different leukemia cell lines. (I, J) Cell viability of parental K562 cells and ABCB1-overexpressing K562 cells upon Doxo (I) and Acla (J) treatment. Data are mean ± SD; *n* = 3 biological replicates; two-way ANOVA. (K) Relative IC_{50} folds of each condition compared to that of Doxo in parental K562 cells. Data are mean ± SEM; *n* = 3 biological replicates; Student's *t*-test. **P* < 0.05, ***P* < 0.01, ****P* < 0.001, and *****P* < 0.0001; n.s., not significant.

Figure 2. Epigenetic selectivity of TopoIIα redistribution and histone eviction of anthracyclines. (A) Illustration of drug-specific TopoIIα redistribution revealed by ChIP-seq. (B) Principal component analysis (PCA) of TopoIIα ChIP-seq data. Two independent biological replicates were included for each condition. (C) Heatmap of TopoIIα peak abundance associated with specific histone features derived from Roadmap Epigenomics Project. (D) Illustration of drug-specific accessible chromatin regions revealed by ATAC-seq. (E)

679 PCA analysis of ATAC-seq data. Two independent biological replicates were included for each condition. (F)
680 Heatmap of ATAC peak abundance associated with specific histone. (G) Density plots showing the accessible
681 and inaccessible TopoIIα regions, and TopoIIα-excluded accessible regions surrounding ±2 kb from the center
682 of the detected peaks in the untreated K562 cells. (H) The abundance of each category in different conditions.
683
684 **Figure 3. Bio-distribution of clinically-used anthracyclines in mice.** (A) Drug bio-distribution was
685 determined 4 hours after i.v. injection of indicated drug at 5 mg/kg. Data are represented as mean ± SD from 5
686 mice per group. Student's *t*-test. (B) Representative microscopic images of γH2AX IHC staining of the hearts.
687 Scale bars, 100 μm. Quantification is represented as mean ± SD, $n = 5$, Mann-Whitney test. *$P < 0.05$, **$P <$
688 0.01, ***$P < 0.001$, and ****$P < 0.0001$; n.s., not significant.
689
690 **Figure 4. Acla is safe and well tolerated following Doxo treatment.** (A) Wild-type FVB mice were i.v.
691 injected with Doxo (D), Acla (A), or saline (C) as indicated. (B E) Representative microscopic images of the
692 left atrium (LA) of heart. Lesions caused by Doxo treatment represent as impairment of the wall, thrombosis,
693 inflammation, fibrosis/calcification, and disappearing of the lumen of atrium (filled by a large thrombus). Scale
694 bars, 500 μm. (F H) Quantification of the indicated IHC staining in LA. Data are mean ± SEM, Mann-
695 Whitney test. (I) Animal survival is plotted in Kaplan-Meier curves. Log-rank test. (J) Cumulative incidence of
696 cardiotoxicity. Fisher's exact test. (K) Incidence rate of cardiotoxicity. Two-way ANOVA with repeated
697 measures, two-sided. *$P < 0.05$, **$P < 0.01$, ***$P < 0.001$, and ****$P < 0.0001$; n.s., not significant.
698
699 **Figure 5. CAG is effective in treating r/rAML patients.** (A) The therapy overview of Ruijin AML cohort.
700 CAG: cytarabin, aclarubicin, G-CSF; IA: idarubicin, cytarabine; VA: venetoclax, azacitidine; Others:
701 chemotherapy regimens other than CAG. (B) Overall survival of the r/rAML patients from the start of r/rAML
702 induction treatment to the date of death. Log-rank test. (C) The statistical analysis of OS of r/rAML patients at 2
703 years. Data are n/N (%), * compared with 2nd-line CAG group, † Fisher's exact test, ‡ Log-rank test, § Mantel-
704 Haenszel test, # compared with 2nd-line CAG patients with favorable and intermediate cytogenetics. (D) Event-
705 free survival of the r/rAML patients from the start of r/rAML induction treatment to the date of
706 relapse/refractory/death. (E) The statistical analysis of EFS of r/rAML patients at 2 years. Data are n/N (%), *
707 compared with 2nd-line CAG group, † Fisher's exact test, ‡ Log-rank test, § Mantel-Haenszel test, # compared
708 with 2nd-line CAG patients with favorable and intermediate cytogenetics.

Figure 1

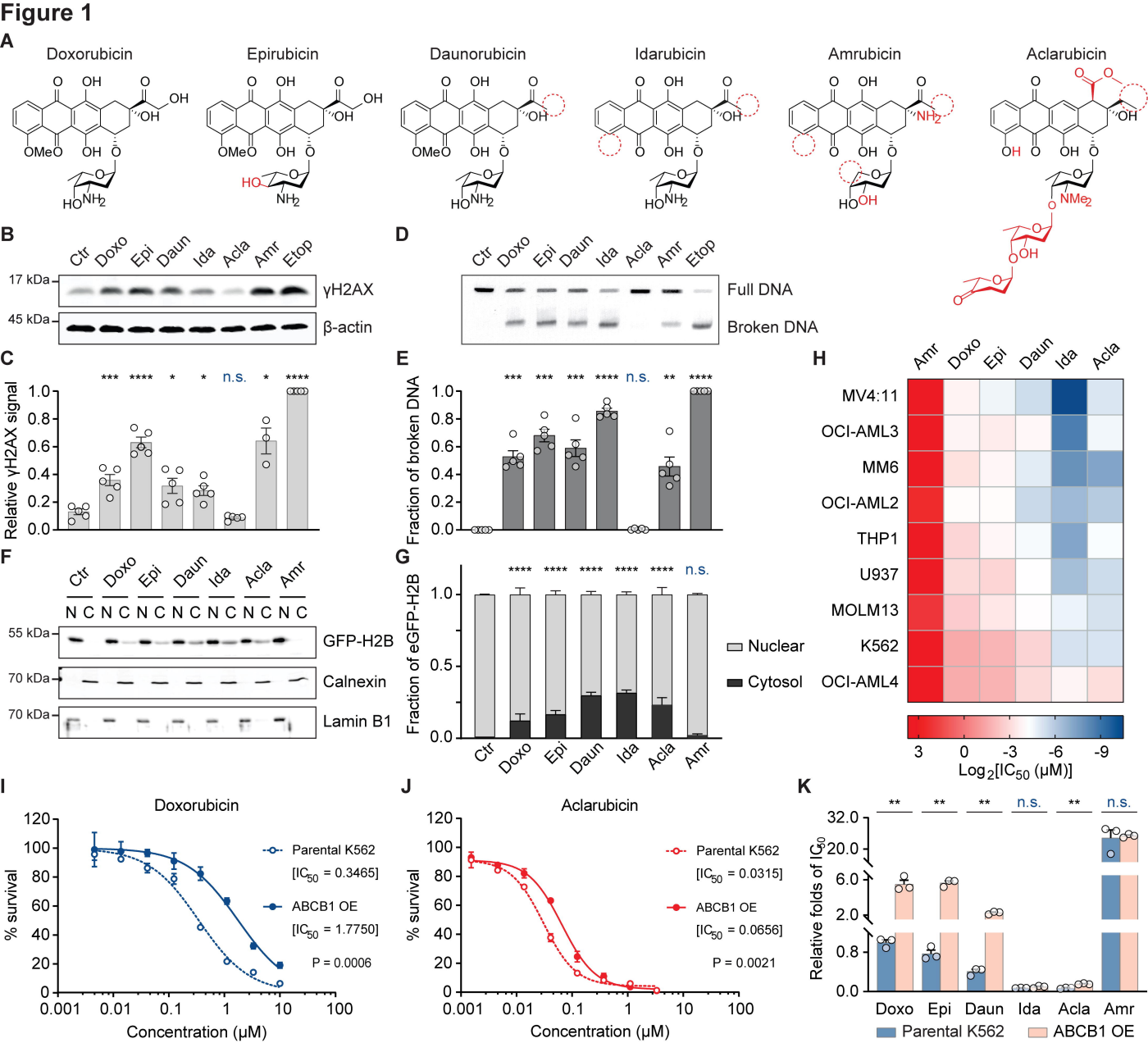
A
Doxorubicin
Epirubicin
Daunorubicin
Idarubicin
Amrubicin
Aclarubicin
B
Ctr Doxo Epi Daun Ida Acla Amr Etop
17 kDa
γH2AX
45 kDa
β-actin
D
Full DNA
Broken DNA
C
Relative γH2AX signal
E
Fraction of broken DNA
H
MV4:11
OCI-AML3
MM6
OCI-AML2
THP1
U937
MOLM13
K562
OCI-AML4
Log2[IC50 (μM)]
F
N C
55 kDa
GFP-H2B
70 kDa
Calnexin
70 kDa
Lamin B1
G
Fraction of eGFP-H2B
Nuclear
Cytosol
I
Doxorubicin
% survival
Parental K562
[IC50 = 0.3465]
ABCB1 OE
[IC50 = 1.7750]
P = 0.0006
Concentration (μM)
J
Aclarubicin
[IC50 = 0.0315]
[IC50 = 0.0656]
P = 0.0021
K
Relative folds of IC50
Parental K562
ABCB1 OE

Figure 2

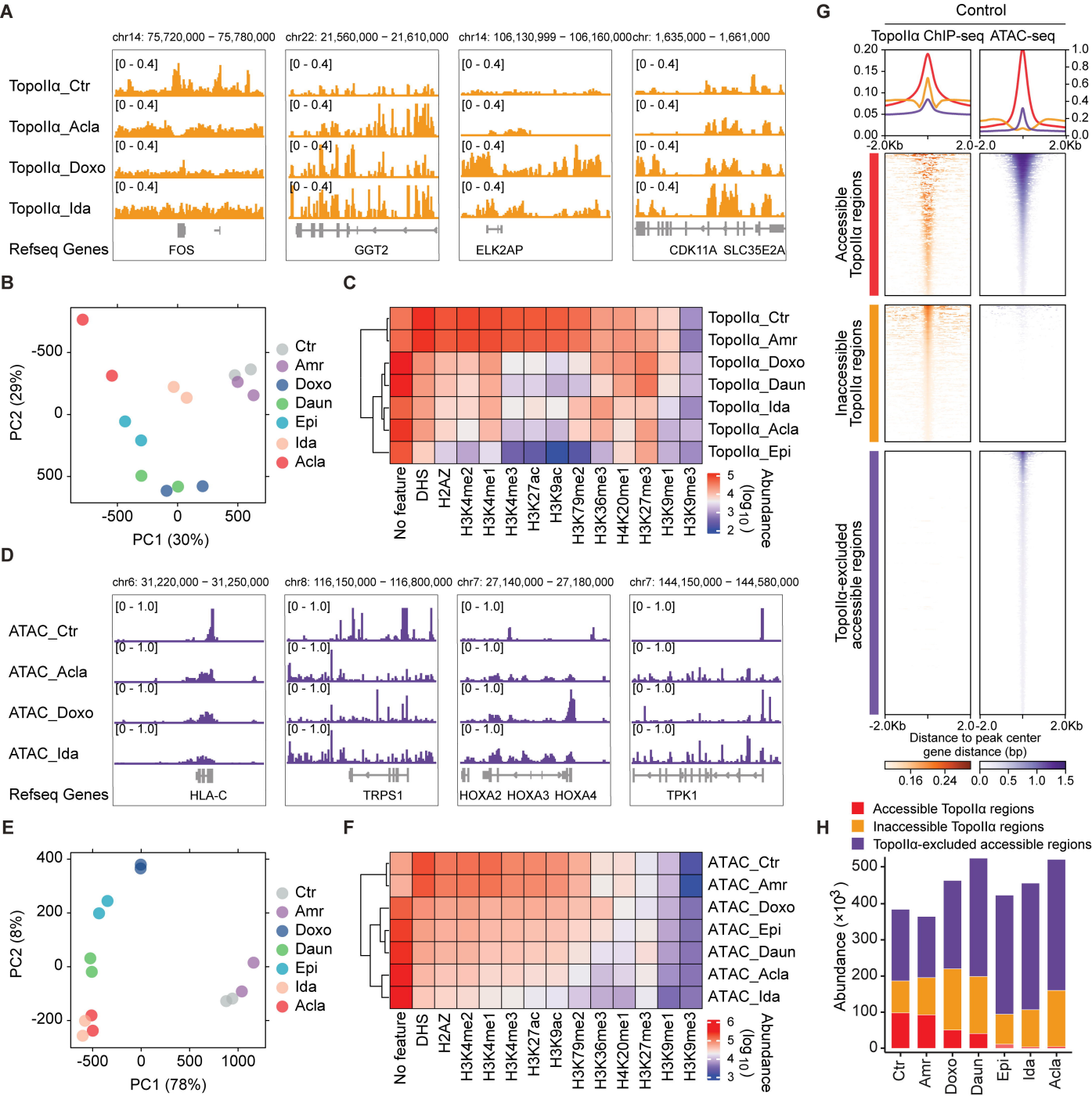
A
chr14: 75,720,000 – 75,780,000
chr22: 21,560,000 – 21,610,000
chr14: 106,130,999 – 106,160,000
chr: 1,635,000 – 1,661,000
[0 - 0.4]
TopoIIα_Ctr
TopoIIα_Acla
TopoIIα_Doxo
TopoIIα_Ida
Refseq Genes
FOS
GGT2
ELK2AP
CDK11A SLC35E2A
B
PC2 (29%)
PC1 (30%)
Ctr
Amr
Doxo
Daun
Epi
Ida
Acla
C
TopoIIα_Ctr
TopoIIα_Amr
TopoIIα_Doxo
TopoIIα_Daun
TopoIIα_Ida
TopoIIα_Acla
TopoIIα_Epi
No feature
DHS
H2AZ
H3K4me2
H3K4me1
H3K4me3
H3K27ac
H3K9ac
H3K79me2
H3K36me3
H4K20me1
H3K27me3
H3K9me1
H3K9me3
Abundance (log10)
D
chr6: 31,220,000 – 31,250,000
chr8: 116,150,000 – 116,800,000
chr7: 27,140,000 – 27,180,000
chr7: 144,150,000 – 144,580,000
[0 - 1.0]
ATAC_Ctr
ATAC_Acla
ATAC_Doxo
ATAC_Ida
Refseq Genes
HLA-C
TRPS1
HOXA2 HOXA3 HOXA4
TPK1
E
PC2 (8%)
PC1 (78%)
Ctr
Amr
Doxo
Daun
Epi
Ida
Acla
F
ATAC_Ctr
ATAC_Amr
ATAC_Doxo
ATAC_Epi
ATAC_Daun
ATAC_Acla
ATAC_Ida
No feature
DHS
H2AZ
H3K4me2
H3K4me1
H3K4me3
H3K27ac
H3K9ac
H3K79me2
H3K36me3
H4K20me1
H3K27me3
H3K9me1
H3K9me3
Abundance (log10)
G
Control
TopoIIα ChIP-seq
ATAC-seq
-2.0Kb
2.0Kb
Accessible TopoIIα regions
Inaccessible TopoIIα regions
TopoIIα-excluded accessible regions
Distance to peak center
gene distance (bp)
H
Accessible TopoIIα regions
Inaccessible TopoIIα regions
TopoIIα-excluded accessible regions
Abundance (×10³)
Ctr
Amr
Doxo
Daun
Epi
Ida
Acla

Figure 3

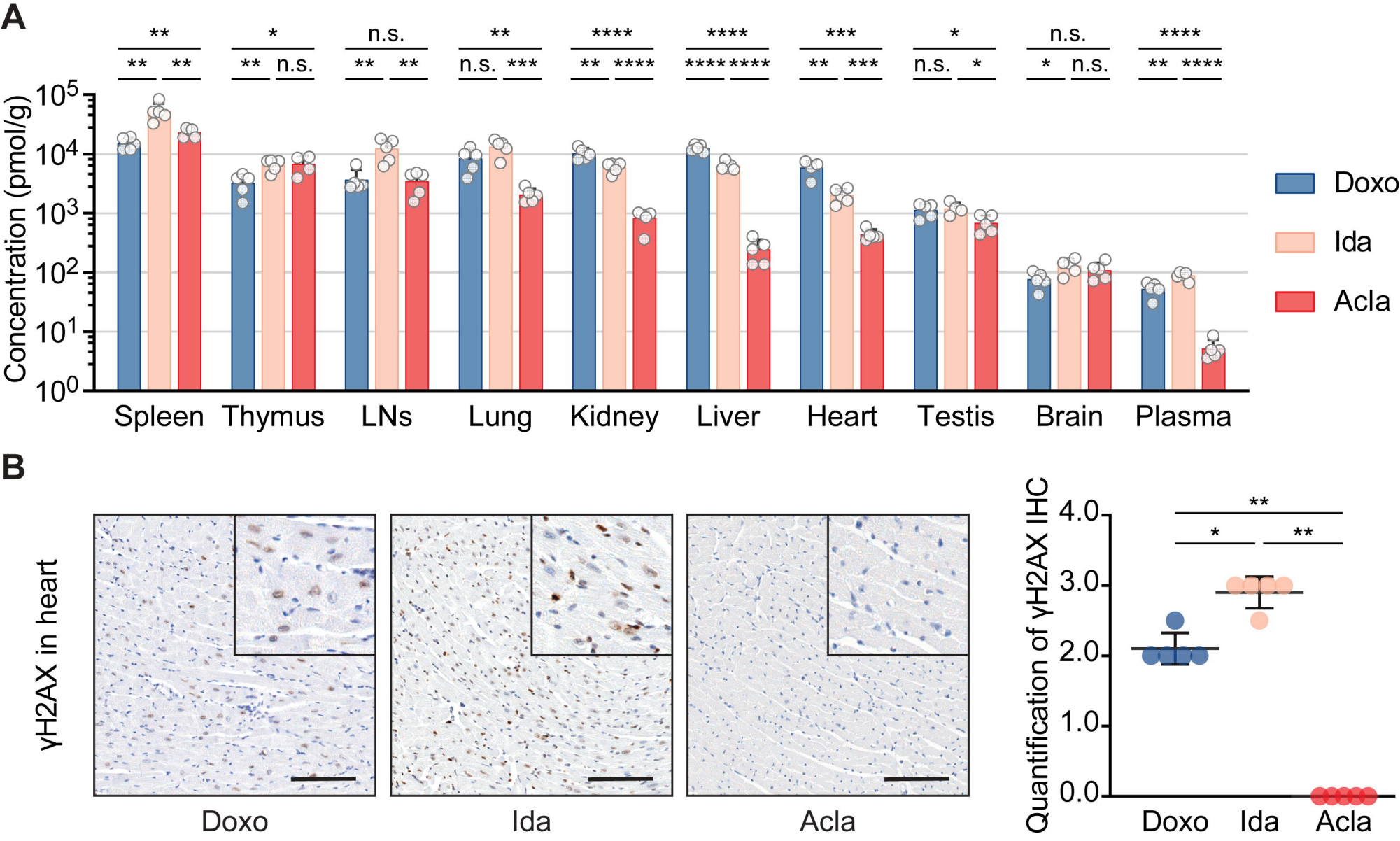
A
**
*
n.s.
**
****
****
***
*
n.s.
****
** **
** n.s.
** **
n.s. ***
** ****
**** ****
** ***
n.s. *
* n.s.
** ****
Concentration (pmol/g)
10^5
10^4
10^3
10^2
10^1
10^0
Spleen
Thymus
LNs
Lung
Kidney
Liver
Heart
Testis
Brain
Plasma
Doxo
Ida
Acla
B
γH2AX in heart
Doxo
Ida
Acla
Quantification of γH2AX IHC
4.0
3.0
2.0
1.0
0.0
**
*
**
Doxo
Ida
Acla

Figure 4

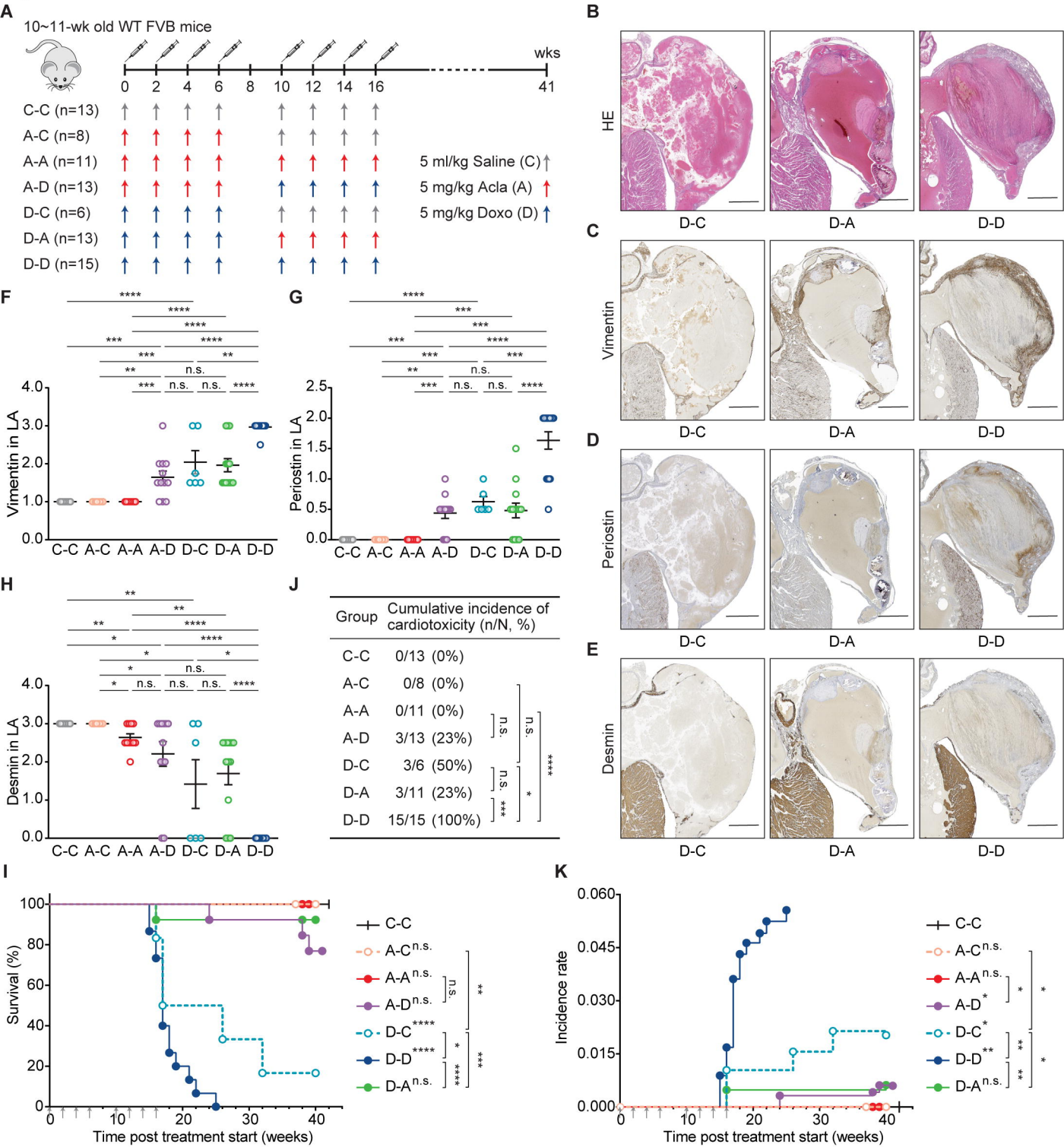
A
10~11-wk old WT FVB mice
wks
0 2 4 6 8 10 12 14 16 41
C-C (n=13)
A-C (n=8)
A-A (n=11)
A-D (n=13)
D-C (n=6)
D-A (n=13)
D-D (n=15)
5 ml/kg Saline (C)
5 mg/kg Acla (A)
5 mg/kg Doxo (D)
B
HE
C
Vimentin
D
Periostin
E
Desmin
D-C
D-A
D-D
F
Vimentin in LA
G
Periostin in LA
H
Desmin in LA
C-C A-C A-A A-D D-C D-A D-D
J
Group
Cumulative incidence of cardiotoxicity (n/N, %)
C-C 0/13 (0%)
A-C 0/8 (0%)
A-A 0/11 (0%)
A-D 3/13 (23%)
D-C 3/6 (50%)
D-A 3/11 (23%)
D-D 15/15 (100%)
I
Survival (%)
Time post treatment start (weeks)
K
Incidence rate
Time post treatment start (weeks)

Figure 5

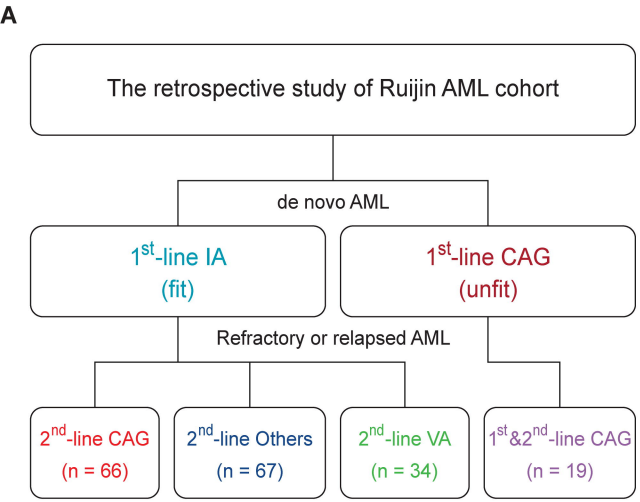

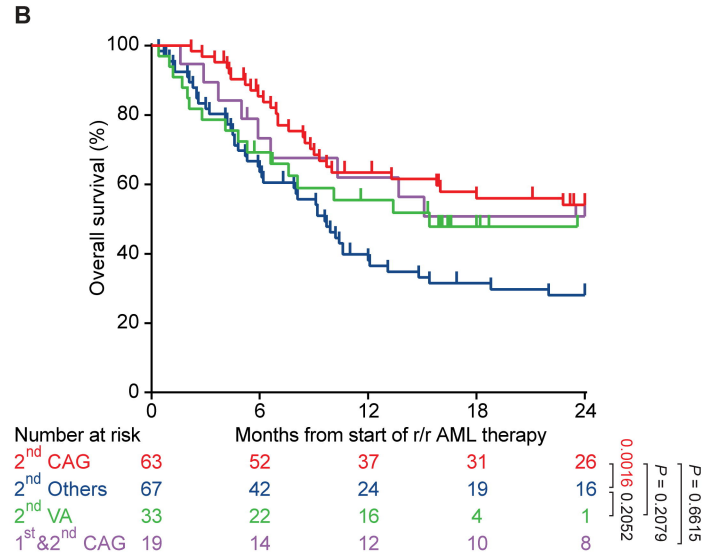

C

OS of r/rAML at 2 years	2nd-line CAG		2nd-line Others		2nd-line VA		1st&2nd-line CAG	
Overall		P value#		P value*		P value*		P value*
Survival	36/63 (57%)		21/67 (31%)	0.0045†	17/33 (52%)	0.6681†	10/19 (53%)	0.7952†
Median time (month)	NA		9.6	0.0016‡	15.4	0.2079‡	NA	0.6615‡
Hazard Ratio (95% CI)			2.109 (1.327 – 3.353)§		1.535 (0.7880 – 2.988)§		1.193 (0.5414 – 2.629)§	
Favourable and intermediate cytogenetics								
Survival	29/48 (60%)		17/58 (29%)	0.0017†	15/27 (56%)	0.8078†	7/14 (50%)	0.5475†
Median time (month)	NA		9.2	0.0004‡	NA	0.2901‡	15.1	0.4251‡
Hazard Ratio (95% CI)			2.538 (1.522 – 4.232)§		1.521 (0.6995 – 3.306)§		1.474 (0.5683 – 3.822)§	
Unfavourable cytogenetics								
Survival	4/11 (36%)	0.1873†	3/7 (43%)	>0.9999†	1/5 (20%)	>0.9999†	1/3 (33%)	>0.9999†
Median time (month)	9.3	0.0698‡	10.2	0.7269‡	4.8	0.4112‡	5	0.6809‡
Hazard Ratio (95% CI)	2.758 (0.9213 – 8.255)§		0.8071 (0.2424 – 2.687)§		1.769 (0.4538 – 6.894)§		1.441 (0.2525 – 8.225)§	

D

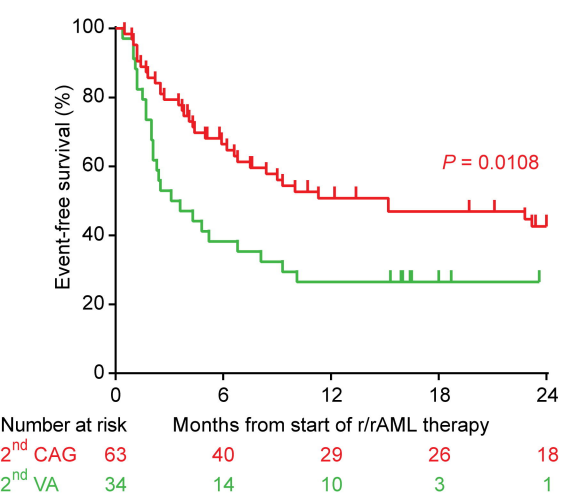

E

EFS of r/rAML at 2 years	2nd-line CAG		2nd-line VA	
Overall		P value#		P value*
Survival	29/63 (46%)		9/34 (26%)	0.0813†
Median time (month)	15.2		3.35	0.0108‡
Hazard Ratio (95% CI)			2.121 (1.190 – 3.782)§	
Favourable and intermediate cytogenetics				
Survival	23/48 (48%)		8/27 (30%)	0.1478†
Median time (month)	22.8		3.6	0.0166‡
Hazard Ratio (95% CI)			2.273 (1.161 – 4.449)§	
Unfavourable cytogenetics				
Survival	3/11 (27%)	0.3162†	1/5 (20%)	>0.9999†
Median time (month)	4.3	0.0684‡	1.7	0.7396‡
Hazard Ratio (95% CI)	2.543 (0.9318 – 6.942)§		1.212 (0.3493 – 4.207)§	

Diverging the anthracycline class of anti-cancer drugs for superior survival of AML patients

Anthracyclines

Cross-resistance

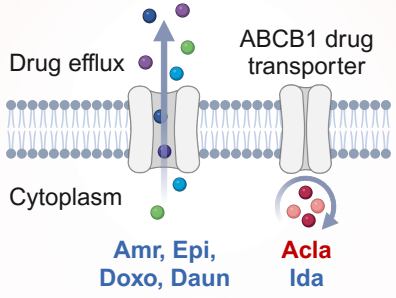

Histone eviction TopoII redistribution

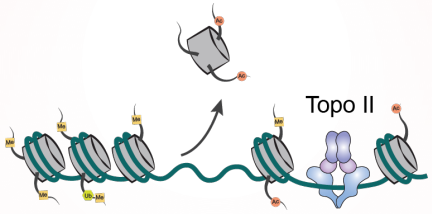

DNA double-strand break

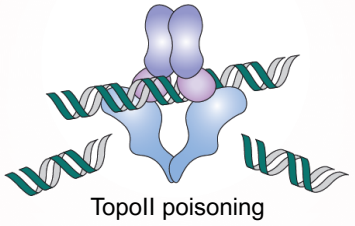

Aclarubicin

Doxo-, Dauno-, Epi- & Idarubicin

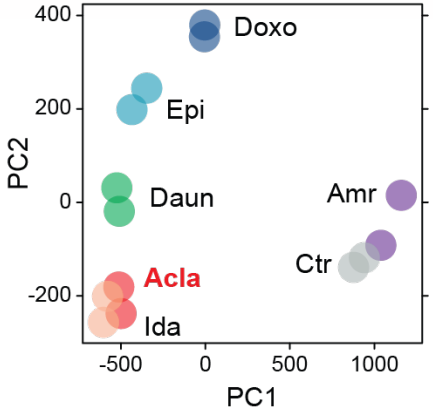

Drug-specific epigenetic regulation

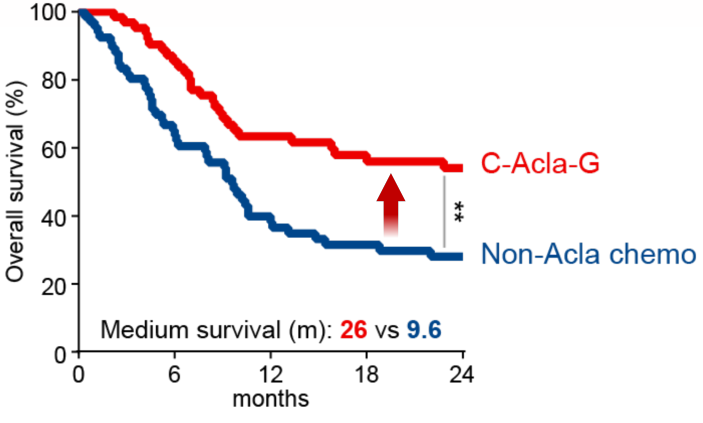

OS of r/rAML

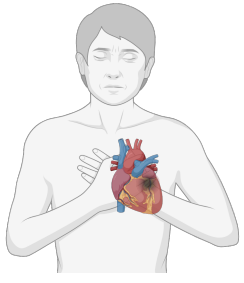

Cardiotoxicity

Considering individual anthracyclines as different drugs can markedly improve survival of AML patients while reducing the toxic side-effects.